TALEN-mediated targeting of HPV oncogenes ameliorates HPV-related cervical malignancy

Zheng Hu,[1] Wencheng Ding,[1] Da Zhu,[1] Lan Yu,[1] Xiaohui Jiang,[1] Xiaoli Wang,[1] Changlin Zhang,[1] Liming Wang,[1] Teng Ji,[1] Dan Liu,[1] Dan He,[2] Xi Xia,[3] Tao Zhu,[1] Juncheng Wei,[1] Peng Wu,[1] Changyu Wang,[1] Ling Xi,[1] Qinglei Gao,[1] Gang Chen,[1] Rong Liu,[1] Kezhen Li,[1] Shuang Li,[1] Shixuan Wang,[1] Jianfeng Zhou,[1] Ding Ma,[1] and Hui Wang[1]

[1]Cancer Biology Research Center and [2]Department of Neurology, Tongji Hospital, Tongji Medical College, Huazhong University of Science and Technology (HUST), Wuhan, Hubei, China.

[3]Center for Reproductive Medicine, Peking University Shenzhen Hospital, Shenzhen, Guangdong, China.

Persistent HPV infection is recognized as the main etiologic factor for cervical cancer. HPV expresses the oncoproteins E6 and E7, both of which play key roles in maintaining viral infection and promoting carcinogenesis. While siRNA-mediated targeting of *E6* and *E7* transcripts temporarily induces apoptosis in HPV-positive cells, it does not eliminate viral DNA within the host genome, which can harbor escape mutants. Here, we demonstrated that specifically targeting *E6* and *E7* within host DNA with transcription activator–like effector nucleases (TALENs) induces apoptosis, inhibits growth, and reduces tumorigenicity in HPV-positive cell lines. TALEN treatment efficiently disrupted *E6* and *E7* oncogenes, leading to the restoration of host tumor suppressors p53 and retinoblastoma 1 (RB1), which are targeted by E6 and E7, respectively. In the K14-HPV16 transgenic mouse model of HPV-driven neoplasms, direct cervical application of HPV16-*E7*–targeted TALENs effectively mutated the *E7* oncogene, reduced viral DNA load, and restored RB1 function and downstream targets transcription factor E2F1 and cycling-dependent kinase 2 (CDK2), thereby reversing the malignant phenotype. Together, the results from our study suggest that TALENs have potential as a therapeutic strategy for HPV infection and related cervical malignancy.

Introduction

Cervical cancer remains the third most common cancer in women worldwide, with approximately 529,800 new cases and 275,100 deaths annually (1, 2). HPVs, especially HPV16 and HPV18, are the main causal factors for the development of cervical cancer. The double-stranded DNA viruses encode 2 primary oncoproteins, E6 and E7, for the maintenance of infection; each gene product has multiple cellular targets. For instance, E6 binds and degrades tumor suppressor p53 and proapoptotic protein BAK, thereby increasing host-cell resistance to apoptosis and permitting viral DNA replication (3, 4). E6 also activates human telomerase reverse transcriptase (5) and SRC-family kinases (6), which provide additional growth advantages to the infected cells during the malignant transformation process. On the other hand, E7 inhibits tumor suppressor retinoblastoma 1 (RB1) to release E2F transcription factors, stimulates cyclin-dependent kinase 2 (CDK2)/cyclin A (7) as well as CDK2/cyclin E complex (8), thus abrogating cell cycle arrest and stimulating proliferation (9). These pivotal roles of *E6* and *E7* in HPV-driven carcinogenesis make them attractive targets for therapeutic interventions.

Previous researchers (including those from our laboratory) have shown that targeting HPV *E6/E7* mRNAs with siRNA could effectively knock down their expression and induce apoptotic cell death in HPV-positive cell lines (10, 11). However, siRNAs only block HPV *E6/E7* mRNAs temporally, and they do not attack the HPV DNA in the nuclei, which serves as a store of escape mutants that cause resistance to siRNA application. In this study, instead of targeting RNA, we designed and optimized transcription activator–like effector nucleases (TALENs) to directly cleave the DNA sequences of oncogenes *E6* and *E7*, both of which are essential for viral functions of either the episomal form (in initial infected cells) or the integrated form (in malignant cells) of the HPV genome (Figure 1A). Theoretically, double-stranded DNA breaks generated by TALEN cleavage would be repaired by the nonhomologous end-joining pathway, resulting in disruption of target oncogenes *E6/E7* and the elimination of HPV infections (Supplemental Figure 1; supplemental material available online with this article; doi:10.1172/JCI78206DS1).

Here, we show for the first time that genome editing of HPV oncogenes *E6/E7* by TALENs efficiently reduced viral DNA load, restored the function of tumor suppressor p53/RB1, and reversed the malignant phenotype of host cells both in vitro and in vivo. Our data provide new insights into drug development for HPV-persistent infections and their related diseases.

Results

Screening and optimization of TALENs with different DNA-binding sites and different architectures. In theory, an ideal TALEN design strategy for knocking out oncogenes E6/E7 is to select binding sites nearest to the 5′ end of the coding sequence. Thus, the double-strand break–induced (DSB-induced) frameshift mutations will affect the entire coding region thereafter. To screen TALENs with the best DNA-targeting efficiency, we designed 8 pairs of TALENs for HPV16 and 8

Authorship note: Zheng Hu and Wencheng Ding contributed equally to this work.
Conflict of interest: The authors have declared that no conflict of interest exists.
Submitted: July 29, 2014; **Accepted:** November 10, 2014.
Reference information: *J Clin Invest*. 2015;125(1):425–436. doi:10.1172/JCI78206.

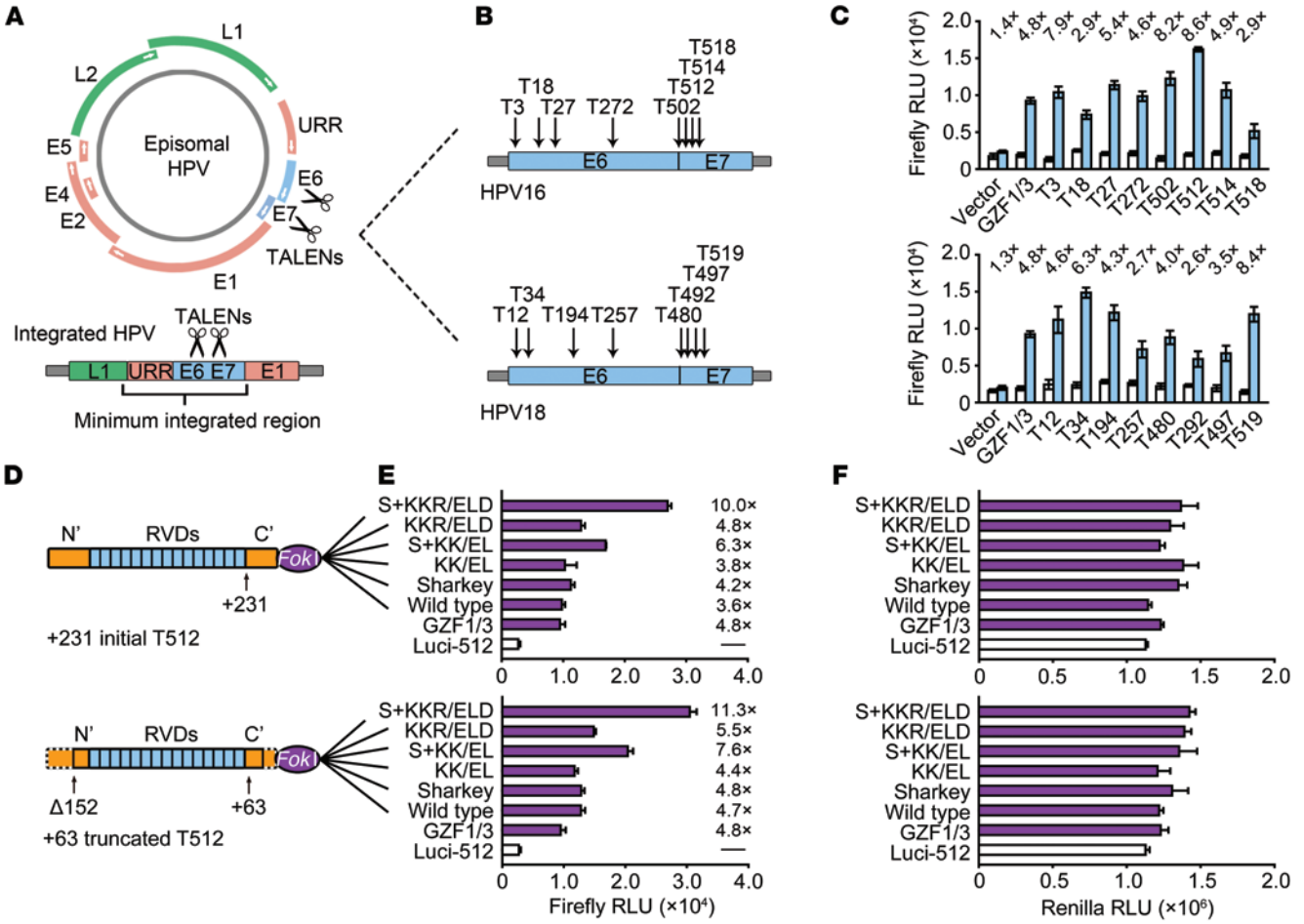

Figure 1. Screening of TALENs with different DNA-binding sites, TALEN architectures, and *Fok*I variants. (**A**) Schematic presentation of the TALEN-mediated disruption of HPV oncogenes. The circular genome represents the episomal HPV genome, and the linear genome represents the integrated HPV genome. URR, upstream regulation region. (**B**) The locations of TALEN DNA-binding sites for HPV16 and HPV18 are indicated by arrows. The numbers in the names of TALENs indicate the first base of the TALEN spacer region. (**C**) Targeting efficiencies of the shown TALENs were measured using the SSA reporter assay. The fold inductions of the TALENs relative to the controls are shown at the top of the columns. RLU, relative luminescence unit. Data represent mean ± SD; $n = 3$ per group. (**D**) Schematic diagram of the initial +231 T512 and the +63 truncated T512 architectures and *Fok*I variants. (Detailed sequences of *Fok*I variants can be found in Supplemental Note 1.) (**E**) The corresponding nuclease activities of these combinations, as measured using the SSA reporter assay. The fold inductions of the TALENs relative to the control, Luci-512, are shown on the right of the columns. The ZFN GZF1/3 was used as a positive control, and the fold induction was related to that of pSSA rep3-1. RVDs, repeat variable diresidues. Data represent mean ± SD; $n = 3$ per group. (**F**) The toxicity profiles of the combinations shown were assessed using the SSA reporter assay. Renilla luminescence signals were constitutively high in the absence of TALEN/ZFN toxicity. Data represent mean ± SD; $n = 3$ per group. All experiments were performed in triplicate.

pairs of TALENs for HPV18 (Figure 1B and Supplemental Table 1). As demonstrated using the single-strand annealing (SSA) reporter system (12), all 16 pairs of TALENs processed nuclease activities to various extents (Figure 1C). HPV16-E6-T27 (5.4-fold increase), HPV16-E7-T512 (8.6-fold increase), HPV18-E6-T34 (6.3-fold increase), and HPV18-E7-T519 (8.4-fold increase) were selected for further investigation because they showed relatively higher cleavage efficiencies than the other pairs.

To further optimize TALENs with high efficiency and low toxicity, different effects of various TALEN architectures and *Fok*I variants should be taken into consideration. The +231 truncation Golden Gate backbone (13) and its +63 truncation version (14) were each individually fused to 6 different *Fok*I variants, comprising a total of 12 different combinations (Figure 1D). Repeat-variable diresidue sequence of T512 was constructed into these backbone combinations. As indicated by SSA reporter assay (Figure 1E), *Fok*Is, which carried ELD/KKR (15) and Sharkey mutations (16), generally demonstrated better efficiency than the other variants; when fused with the C-terminal +63 truncation architecture, *Fok*I induced the highest frequency of DNA breaks with comparably low toxicity (Figure 1F). The efficiencies of these combinations were further confirmed using a surrogate reporter system (Supplemental Figure 2 and ref. 17). These data are consistent with a previous report that ELD/KKR mutations demonstrate a synergic effect with Sharkey mutations in a zinc finger nuclease (ZFN) (18); therefore, +63 truncation architectures fused to *Fok*Is containing both ELD/KKR and Sharkey mutations were selected as default backbone for TALENs used in this study. Besides HPV16-E7-T512, 3 other TALENs, HPV16-E6-T27, HPV18-E6-T34, and HPV18-E7-T519, were also cloned into the +63 truncation architectures fused to *Fok*Is containing ELD/KKR and Sharkey mutations.

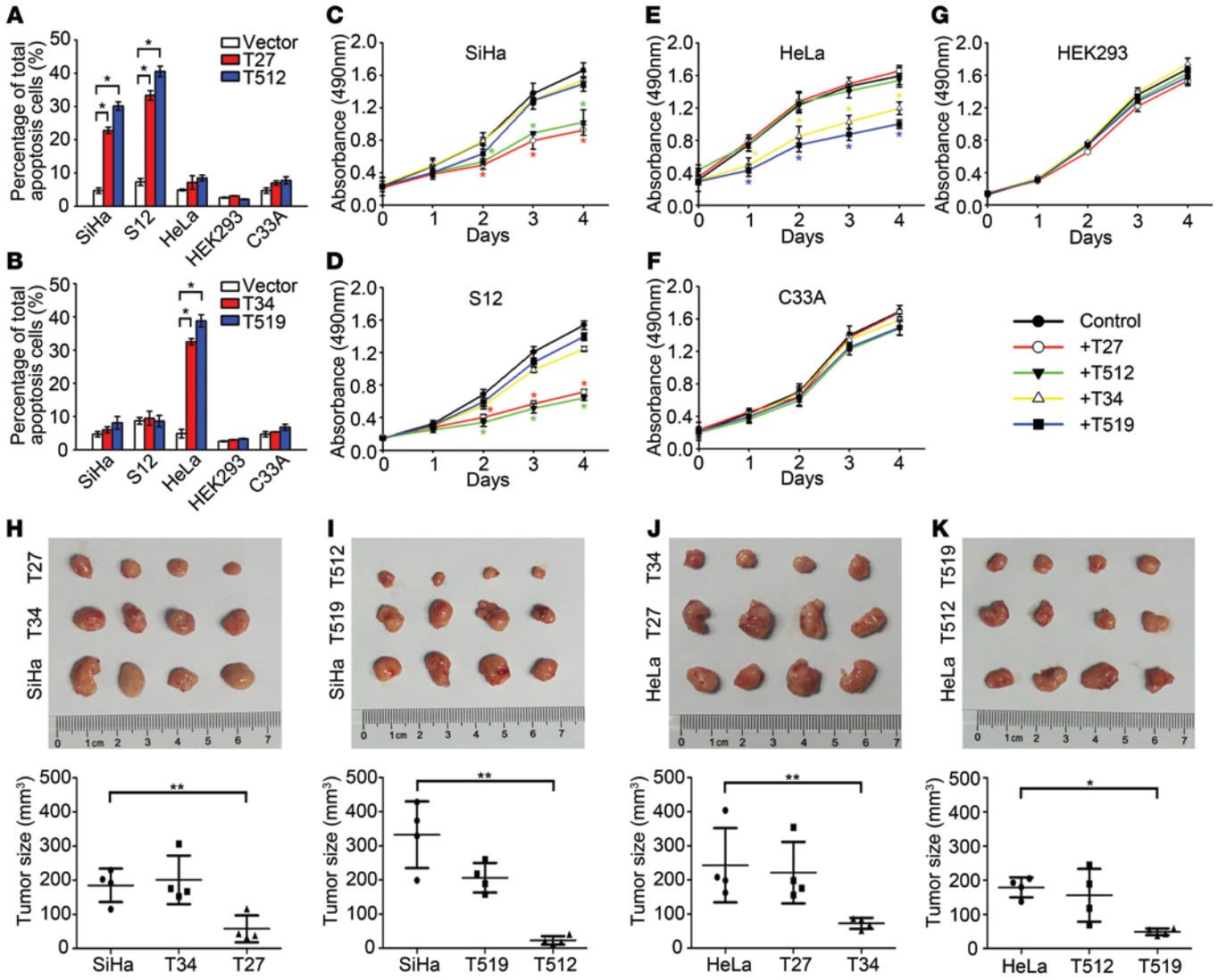

Figure 2. TALENs induce cell apoptosis and arrest growth subtype — specifically in vitro and in vivo. (**A** and **B**) Apoptosis rate of HPV16-positive S12, HPV16-positive SiHa, HPV18-positive HeLa, HPV-negative C33A, and HPV-negative HEK293 cells 48 hours after treatment with (**A**) HPV16-E6-T27 and HPV16-E7-T512 and (**B**) HPV18-E6-T34 and HPV18-E7-T519. Error bars indicate the mean ± SD; $^*P < 0.01$, compared to the untreated cells, 2-tailed Student's *t* test; $n = 3$ per group. (**C**–**G**) Growth curves of TALEN-treated (**C**) SiHa, (**D**) S12, (**E**) HeLa, (**F**) C33A, and (**G**) HEK293 cells were constructed using the CCK-8 assay. All experiments were performed in triplicate. Data represent mean ± SD; $^*P < 0.01$, compared to the untreated cells, 2-tailed Student's *t* test; $n = 3$ per group. (**H**–**K**) Representative images of in vivo xenografts of SiHa and HeLa cells after treatment with TALENs for 30 days in nude mice and the calculated tumor sizes. (**H**) SiHa xenografts after treatment with T34 and T27. (**I**) SiHa xenografts after treatment with T519 and T512. (**J**) HeLa xenografts after treatment with T27 and T34. (**K**) HeLa xenografts after treatment with T512 and T519. The column scatter plots were used to present every data point, and the lines represent mean ± SD; $^*P < 0.05$, $^{**}P < 0.01$, 2-tailed Student's *t* test; $n = 4$ per group.

TALENs targeting HPV E6/E7 specifically induced apoptosis, growth inhibition, and reduction of tumorigenicity in HPV-infected cells. First, the efficacies and specificities of HPV *E6/E7*–targeted TALENs were investigated in our cellular models, which included (a) both HPV-positive and HPV-negative cell lines for monitoring TALEN's effects on cells with and without HPV infections and (b) both HPV16-positive and HPV18-positive cell lines for studying the cross-reactivities of TALENs targeting different subtypes of HPVs. As is shown in Figure 2, A–G, HPV16-targeting TALENs (T27 and T512) specifically induced the apoptosis and inhibited growth of HPV16-positive S12 and SiHa cell lines, while they did not exert effects on the HPV18-infected HeLa cell line (Figure 2, A–G). Similarly, HPV18-targeting TALENs (T34 and T519) specifically induced apoptosis and growth suppression of HPV18-positive cell lines but not HPV16-positive cell lines (Figure 2, A–G). Moreover, HPV16- and HPV18-targeting TALENs demonstrated minimum toxicities on the HPV-negative C33A cell line and human embryonic kidney 293 cells (HEK293) (Figure 2, A–G, and Supplemental Figure 3).

To further validate the therapeutic effects of TALENs in vivo, identical numbers of TALEN-treated SiHa cells or HeLa cells were injected subcutaneously into nude mice. TALEN plasmids were cotransfected with EGFP expression plasmid (pEGFP-C1) to ensure the total transfection efficiency was above 70%. In accordance with in vitro data, SiHa cells treated with T27 and T512 (but not T34 and T519) as well as HeLa cells

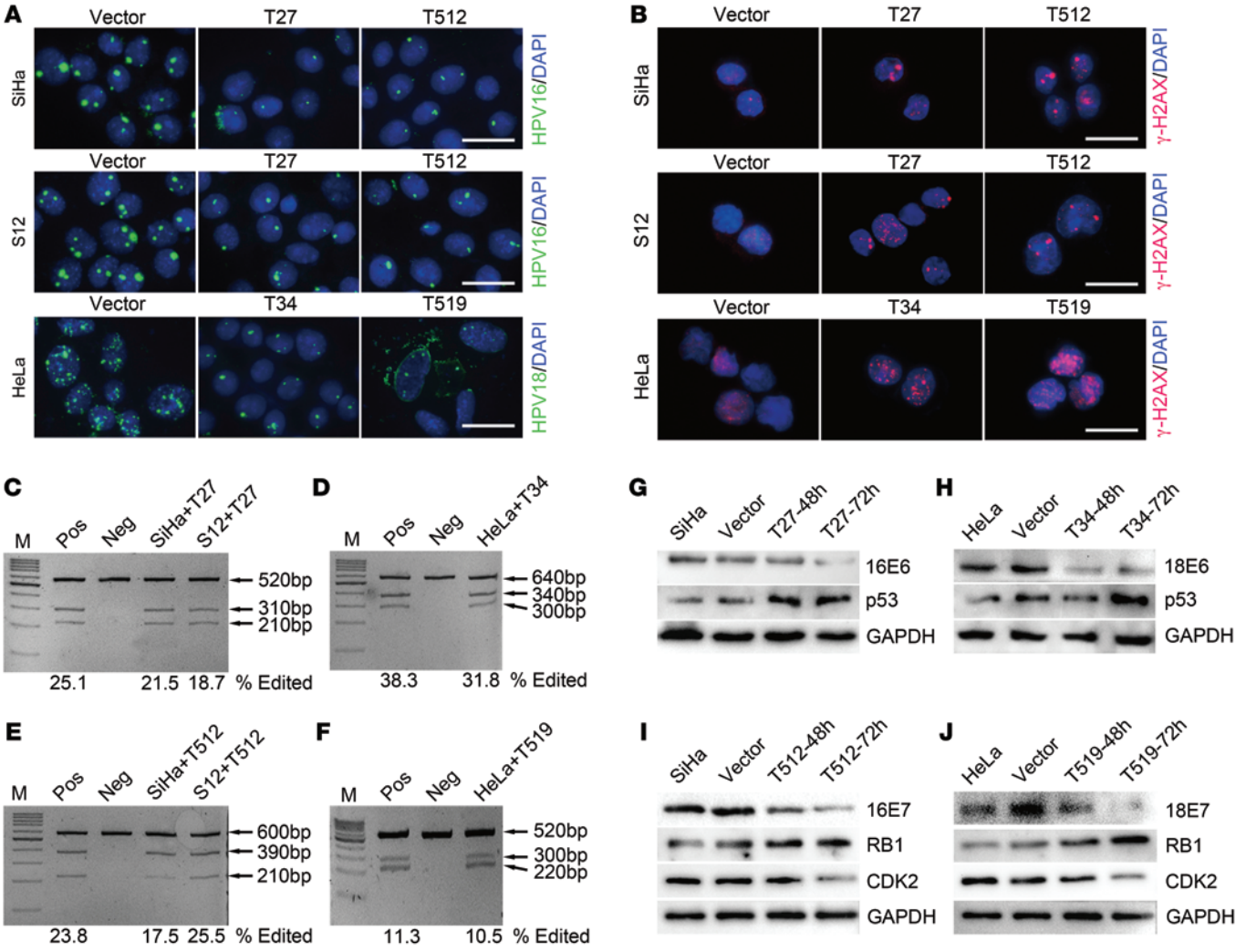

Figure 3. Efficacies of HPV subtype-specific TALENs in HPV-infected, precancerous, and cancer cells. (**A** and **B**) The representative images of (**A**) FISH and (**B**) γ-H2AX foci (red signals) in vector-, T27-, and T512-treated SiHa and S12 cells and in vector-, T34-, and T519-treated HeLa cells. Cell nuclei were indicated by DAPI staining (blue). *n* = 3 per group. Scale bars: 20 μm. (**C**–**F**) Detection of E6/E7 mutations using T7EI assays in SiHa, HeLa, and S12 cells. The sizes of the total PCR fragments (top one) and the cut fragments (bottom two) are marked with arrows. The numbers below the lanes represent the percentage of cleaved PCR products. Pos, T7EI-treated PCR fragments that contained a 2-bp deletion in the middle of the spacer region of the corresponding TALEN were mixed at 1:1 with PCR products that were amplified from TALEN-treated cells. Neg, PCR products that were amplified from TALEN-treated cells and not treated by T7EI. *n* = 3 per group. (**G**–**J**) Western blotting analysis of the E6 and E7 oncoproteins and their downstream proteins in SiHa or HeLa cells 48 and 72 hours after treatment with the corresponding TALENs. (**G**) HPV16 E6 and p53 in SiHa cells after treatment with HPV16-E6-T27. (**H**) HPV18 E6 and p53 in HeLa cells after treatment with HPV18-E6-T34. (**I**) HPV16 E7, RB1, and CDK2 in SiHa cells after treatment with HPV16-E7-T512. (**J**) HPV18 E7, RB1, and CDK2 in HeLa cells after treatment with HPV18-E7-T519. *n* = 3 per group.

treated with T34 and T519 (but not T27 and T512) showed lower rates of xenograft formation and smaller tumor sizes than controls (Figure 2, H–K). Together, these data demonstrated that E6/E7-targeted TALENs showed promising therapeutic efficacy and specificity in HPV-infected cervical cancer cells.

Genome editing of HPV E6/E7 reduced viral DNA load and recovered the expression of p53/RB1. To verify that the therapeutic effects did result from genome editing of HPV *E6/E7*, we visualized TALEN-generated double-stranded DNA breaks by immunofluorescence staining of γ-H2AX, which accumulated at the DSB sites and could be used as a DNA damage marker. We first checked the initial HPV copy numbers of target cell lines by FISH (1–2 copy numbers of HPV16 in SiHa cells, 1–3 copy numbers of HPV16 in S12 cells, and 17–35 copy numbers of HPV18 in HeLa cells based on our results; Figure 3A and Supplemental Figure 4), because they should be approximately in accordance with the foci numbers of γ-H2AX induced by TALENs. A higher number of γ-H2AX foci than the initial copy number of HPV signifies potential off-targets, while the opposite implies inefficient activities of TALENs. As determined by γ-H2AX immunofluorescence staining, after treatment with T27 and T512, the expression of γ-H2AX in the SiHa cells was significantly increased, with the mean number of γ-H2AX foci per nuclei increased from 0.50 ± 0.14 (vector) to 1.60 ± 0.14 (T27) and 1.80 ± 0.12 (T512) (Figure 3B and Supplemental Figure 5). Similar results were obtained in S12 and HeLa cell lines, with the mean number of γ-H2AX foci per nuclei in S12 cells

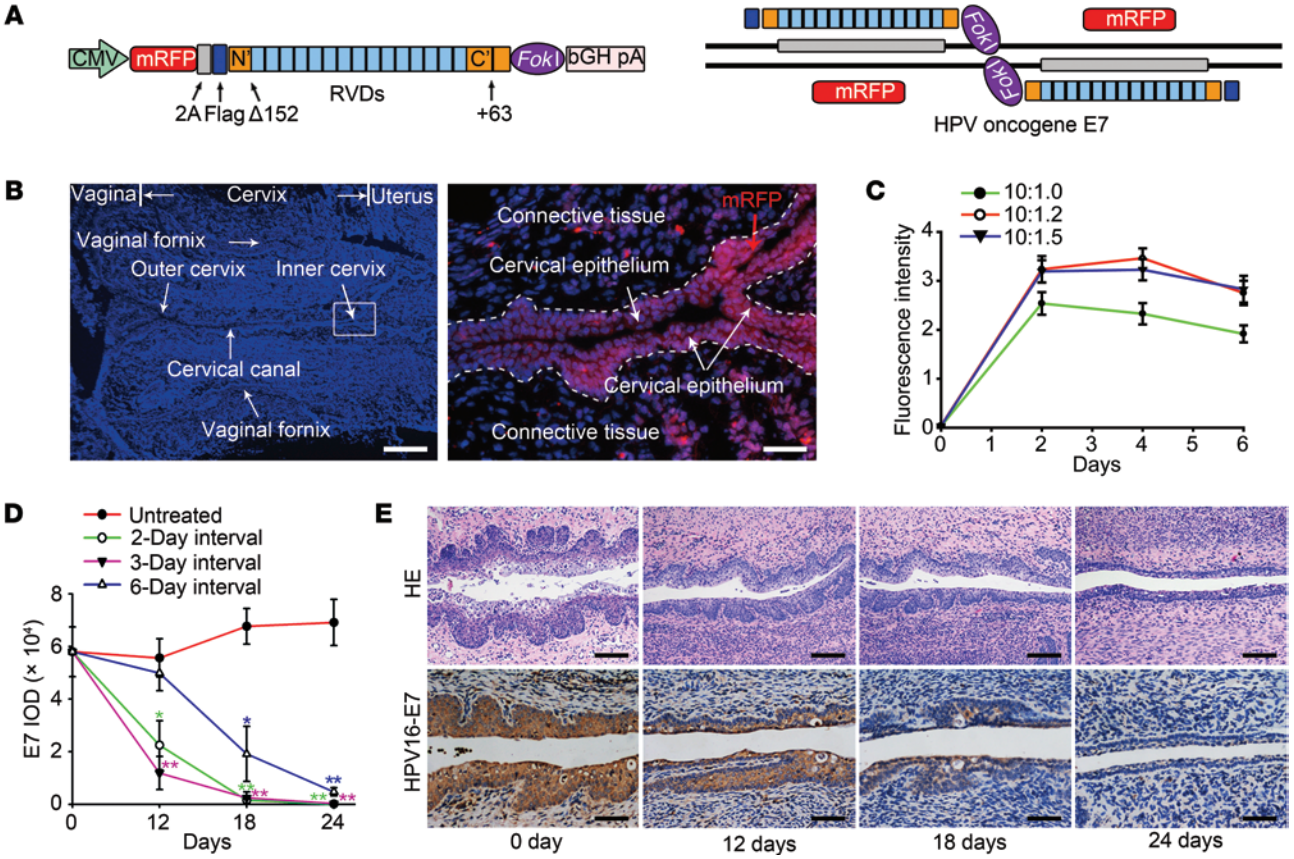

Figure 4. Establishment and optimization of regional TALEN application to the uterine cervixes of K14-HPV16 transgenic mice. (**A**) FLAG-tagged HPV16-E7-T512 was fused with mRFP to monitor its expression and distribution. bGH pA, bovine growth hormone and polyadenylation signal. (**B**) Localized expression of HPV16-E7-T512 in the cervical epithelium. The right panel shows the boxed region in the left panel at higher magnification. Scale bars: 200 μm (left panel); 40 μm (right panel). *n* = 3 per group. (**C**) Optimization of the transfection efficiency through the use of a range of DNA-to-polymer ratios. Ten micrograms of the mRFP expression plasmids that were incubated with the corresponding volumes of polymer were transfected intravaginally. At days 2, 4, and 6, exfoliated cervical cells from the treated mice were gathered (with a process similar to a Pap smear test), and the mRFP-positive cells were counted. Data represent mean ± SD; *n* = 3 for each group of treated mice. (**D**) HPV16-E7-T512 was applied at 2-day, 3-day, or 6-day intervals for 24 days, and the E7 expression levels were assessed using IHC staining at treatment days 0, 12, 18, and 24. The integrated optical density (IOD) values were measured using Image-Pro PLUS (version 6.0). Data represent mean ± SD; $^{*}P < 0.05$, $^{**}P < 0.01$, 2-tailed Student's *t* test; *n* = 3 per group. (**E**) Representative data from H&E staining and E7 IHC staining at treatment days 0, 12, 18, and 24. The mice were treated with HPV16-E7-T512 using the 3-day interval regimen. *n* = 3 per group. Scale bars: 80 μm.

increased from 0.40 ± 0.11 (vector) to 2.65 ± 0.24 (T27) and 2.25 ± 0.24 (T512), and the mean number of γ-H2AX foci per nuclei in HeLa cells increased from 1.15 ± 0.26 (vector) to 19.65 ± 0.74 (T34) and 21.20 ± 1.04 (T519) (Figure 3B and Supplemental Figure 5). The increased γ-H2AX foci numbers of SiHa, S12, and HeLa cells were consistent with the initial copy number observed in the FISH assay (Supplemental Figure 5 and 6). Moreover, we did not observe any increase of γ-H2AX foci in HEK293 cells treated with the above 4 pairs of TALENs (Supplemental Figure 6) or in SiHa, S12, and HeLa cells that received TALENs with different HPV subtype (Supplemental Figure 7). Our data indicate that TALEN-mediated genome editing of HPV E6/E7 in host cells was highly efficient with low off-target rate.

We also applied mismatch-sensitive T7 endonuclease I (T7EI) assays to validate TALEN-induced DNA disruption. The expected cleaved bands were detected by analyzing T7EI-treated PCR amplicons of the HPV16 *E6* gene from T27-treated SiHa and S12 cells (Figure 3C), the HPV18 *E6* gene from T34-treated HeLa cells (Figure 3D), the HPV16 *E7* gene from T512-treated SiHa and S12 cells (Figure 3E), and the HPV18 *E7* gene from T519-treated HeLa cells (Figure 3F). The data confirm the mutagenic activities of the above 4 pairs of TALENs at the genomic level. Of note, T7EI assay could not detect homoduplexes formed by identical mutant sequences and, therefore, may underestimate the mutagenic activities of the above TALENs (17, 19, 20).

Intriguingly, we found that the DNA copy numbers of HPV16 in S12 and SiHa cells were significantly decreased after 2 weeks of treatment with T27 and T512 (Figure 3A and Supplemental Figure 4), and the same phenomenon could be observed in HeLa cells after treatment with T34 and T519 (Figure 3A and Supplemental Figure 4). It can be inferred that the more HPV replicates its DNA, the more likely it gets cleaved by the virus-targeted TALENs. Furthermore, the genotoxicity produced by TALEN cleavage of HPV oncogenes would cause selective apoptosis of the infected host cells and has the potential to eliminate HPV-persistent infections.

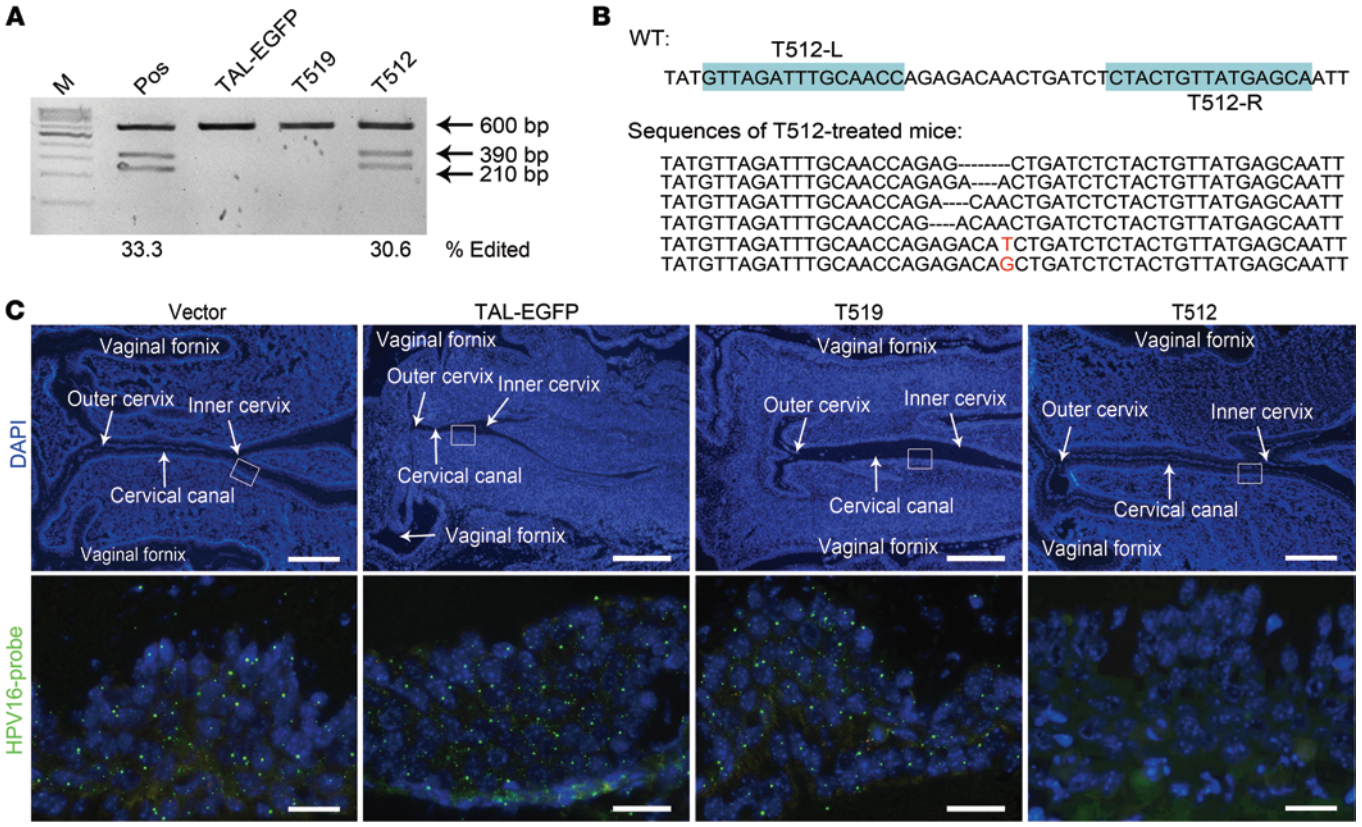

Figure 5. In vivo effects of topical TALEN application in K14-HPV16 transgenic mice. (**A**) T7EI assays were conducted to measure the E7 mutations in TALEN-treated K14-HPV16 transgenic mice at day 24. The size of the PCR fragment was approximately 600 bp, and the endonuclease-digested DNA fragment sizes were approximately 210 bp and 390 bp. The numbers below the lanes represent the percentage of cleaved PCR fragments. *n* = 3 per group. (**B**) Representative sequencing results of mutations induced by HPV16-E7-T512 in cervical epithelium; the DNA-binding sequences of HPV16-E7-T512 are highlighted in blue. The red letters in the sequences represent the detected missense point mutations. (**C**) FISH revealed that HPV16 DNA (punctate green signal) was markedly reduced in the cervical epithelia of HPV16-T512–treated mice compared with that from vehicle-treated mice. The images in the bottom row show the boxed regions from the top row at higher magnification. *n* = 3 per group. Scale bars: 200 μm (top panel); 20 μm (bottom panel).

TALEN-mediated disruption of the viral oncogenes *E6* and *E7* subsequently led to the disruption of their corresponding proteins. As revealed by Western blotting, T27 and T34 could effectively block the expression of HPV16 E6 and HPV18 E6, respectively (Figure 3, G and H), and downregulation of E6 directly restored the expression of tumor suppressor p53. Similarly, T512 and T519 blocked the expression of HPV16 E7 and HPV18 E7, respectively. And an increase in the RB1 protein level was found to accompany the decrease in HPV E7 protein level (Figure 3, I and J). In addition, we found that the expression level of positive cell cycle regulator CDK2 was downregulated with increased RB1 expression levels, suggesting cell cycle arrest in T512- and T519-treated cells (Figure 3, I and J). Thus, TALEN-mediated downregulation of oncoproteins E6/E7 and restoration of p53/RB1 contributed to the therapeutic effects of TALEN on HPV-infected cells.

Repeated topical application of HPV E7–targeted TALENs blocked E7 expression and reversed the malignant phenotype of host cells in a gradual manner. To further investigate the efficacy of TALENs in the animal model with existing HPV infection, we administered polymer-complexed T512 plasmids directly onto the cervixes of K14-HPV16 transgenic mice. This mouse strain uses the human keratinocyte 14 enhancer/promoter to direct the expression of the HPV16 early region (including *E6* and *E7*) in basal keratinocytes. As a result, the model exhibits various degrees of HPV-induced epidermal and squamous mucosal hyperplasia and is an ideal model for HPV-driven cervical carcinogenesis (Supplemental Figure 8 and ref. 21). We fused the N terminus of FLAG-tagged HPV16-E7-T512 with the monomeric red fluorescent protein (cloned from CAG-mRFP plasmid) to monitor the expression and the distribution of the topically applied TALENs (mRFP-T512; Figure 4A). Red fluorescence was observed only in vaginal and cervical epithelium and the connective tissues beneath the basement membrane but not in nearby organs (rectum or remote organs, i.e., heart, liver, lung, or kidney tissues) (Figure 4B and Supplemental Figure 9). The regional localization of mRFP-T512 suggested that topical application of TALENs was a relatively safe approach and that its effect was limited to the vaginal and cervical epithelium, in which HPV infection was established. Generally, red fluorescence peaked from 48 to 96 hours after transfection and lasted for at least 6 days (Figure 4C and Supplemental Figure 10). We tested a range of DNA-to-polymer ratios and plasmid quantities to obtain the best transfection efficiency. Mice were administered 10 μg mRFP-T512 plasmid, with different amounts of polymer (Figure 4C). A mixture of 10 μg mRFP-T512 plasmid with 1.2 μl polymer proved to be optimal (Supplemental Figure 11).

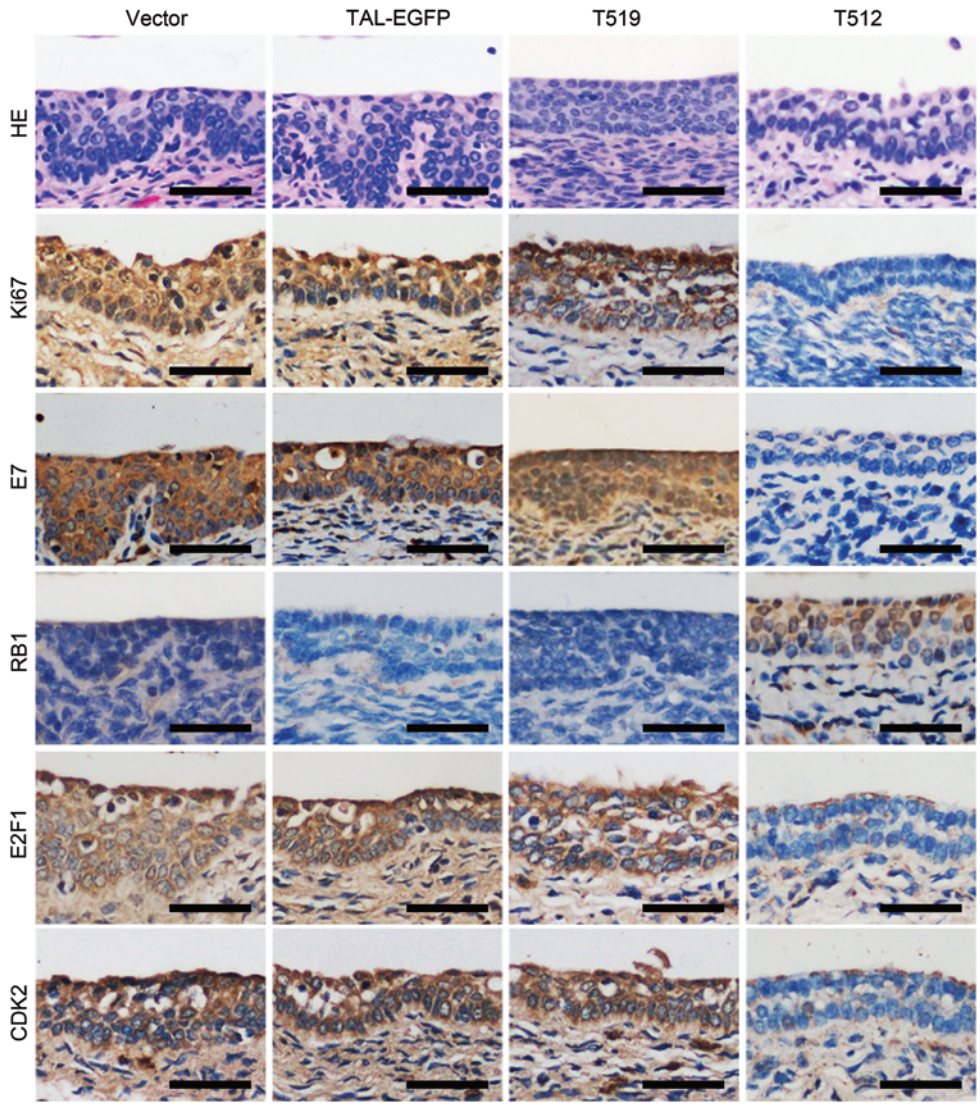

Figure 6. Histopathological changes and protein expression of E7, RB1, Ki67, CDK2, and E2F1 in the cervical tissue from T512-treated mice. To examine the in vivo efficacy of TALEN and the underlying mechanisms involved, we investigated several molecular markers in TALEN-treated transgenic mice. $n = 3$ per group. Scale bars: 80 μm.

To achieve the optimal therapeutic effects, T512 was applied at 2-day, 3-day, or 6-day intervals for a total of 24 days. On day 12, the cervical epithelium of the K14-HPV16 mouse began to show a gradual loss of E7 and a reduction of epithelial proliferation (Figure 4, D and E). On day 24, E7 expression was almost undetectable. In addition, H&E staining showed that cervical intraepithelial neoplasia (CIN) in T512-treated K14-HPV16 mice gradually regressed to normal-appearing cervical epithelia, which also exhibited loss of E7 (Figure 4E). The 3-day interval regimen was chosen for subsequent study because it exhibited an E7 reduction rate similar to that of the 2-day interval regimen but caused less irritation to the vagina and the uterine cervix. To determine the duration of the therapeutic effects, 3 of the T512-treated mice from the 3-day interval regimen were kept without any treatment for another 2 months. In these 3 mice, we did not observe recurrences of the cervical neoplasia, and E7 protein expression was barely detectable in the cervical epithelium (Supplemental Figure 12). Therefore, we think that the duration of the effect on neoplasia would be at least 2 months. Continued observations on such effects are still ongoing in our laboratory to determine whether the neoplasia would recur later.

Topical TALEN application induced E7 mutations and reduced viral DNA load in K14-HPV16 transgenic mice. We next confirmed the DNA mutations in the *E7* gene in mice that received topical T512 for a total of 24 days. Cleaved bands could be observed in T7EI-treated amplicons of the *E7* oncogene in T512-treated transgenic mice, indicating the existence of *E7* mutations (Figure 5A). By cloning and sequencing the *E7* gene in topical T512-treated K14-HPV16 transgenic mice (Figure 5B), we found that the sequences of oncogene *E7* were efficiently edited by T512 treatment, resulting in deletion or point mutations. The effects of topical TALEN application were highly specific: *E7* mutations were not detected in mice treated with HPV18-T519, *EGFP*-targeted TALEN, or vector alone. Further, we did not detect any mutations in the top 10 predicted off-target sites in the mouse genome (ref. 22 and Supplemental Table 2). In addition to detection of DNA mutation, we applied FISH assay to analyze the viral DNA load in cervical epithelia of topical T512-treated K14-HPV16 transgenic mice. In accordance with in vitro data, loss of the HPV DNA load was only observed in the T512-treated group (Figure 5C), not in the control groups, confirming the potential of TALEN to eliminate persistent HPV infections in vivo.

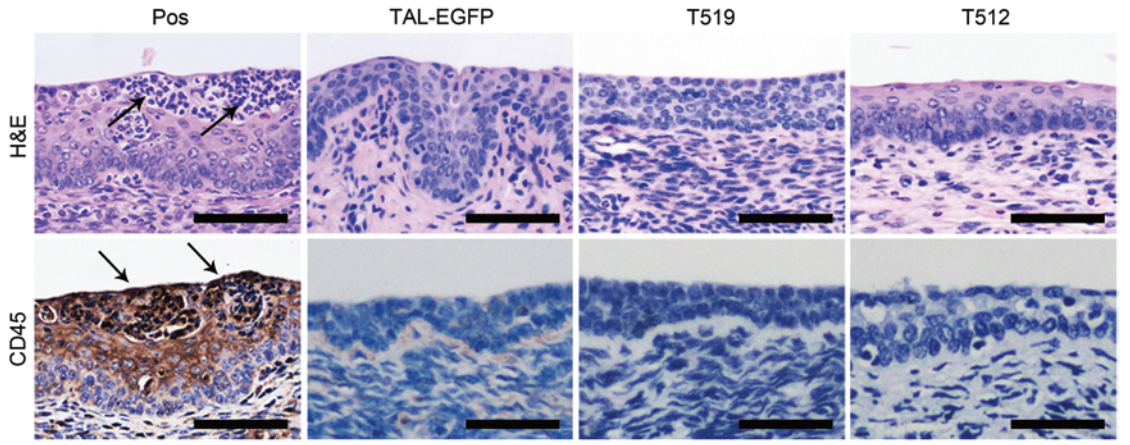

Figure 7. H&E and IHC staining of CD45 to analyze the inflammatory response in T512-treated mice. H&E staining (top) and IHC staining (bottom) of CD45. Pos, mechanically stretched cervical tissue. Arrows represent the inflammatory cells. *n* = 3 per group. Scale bars: 80 μm.

HPV subtype-specific reversal of cervical malignancy and restoration of RB1 function in mice receiving a 24-day TALEN regimen. We then performed H&E staining to observe the morphological changes in the epithelia of mice that were treated with topical TALENs for 24 days. Nuclear atypia and loss of normal squamous maturation could be observed in the cervical epithelia of vector-treated mice, TAL-EGFP–treated (TALENs target *EGFP*) mice, and T519-treated mice but not in the epithelia of T512-treated mice. Instead, CIN in T512-treated mice was replaced with normal-appearing, well-differentiated epithelia (Figure 6).

To further examine the in vivo efficacy of TALEN and the underlying mechanisms involved, we also investigated several molecular markers in TALEN-treated transgenic mice (Figure 6). Compared with the controls, T512-treated K14-HPV16 transgenic mice exhibited a marked loss of HPV16 E7, which led to restored expression of its cellar target tumor suppressor RB1. Moreover, cell cycle regulator E2F1 transcription factors (RB1 downstream target) and CDK2 were markedly downregulated in T512-treated groups, suggesting inhibition of G_1-to-S phase cell cycle entry (23). It could be inferred that RB1 restoration and cell cycle arrest contributed to TALEN-mediated reversal of cervical malignancy, which was indicated by a markedly reduced expression of cellular proliferation marker Ki67 in T512-treated cervical epithelium.

Inflammatory response in T512-treated mice. As TALENs are a special type of DNA-binding protein originated from *Xanthomonas* bacteria (24, 25), one concern is that topical application of TALENs may induce host immune responses and unnecessary inflammation. In this study, H&E staining of the cervical epithelium after 24 days of TALEN treatment (including TAL-EGFP– and T519-treated mice) did not reveal any obvious inflammatory response (Figure 7), such as high leukocytosis in blood vessels or the appearance of mast cells, macrophages, or neutrophils, while, the positive control mice (a normal mouse scratched intravaginally with a syringe needle under anesthesia) demonstrated a cluster of inflammatory cells in both H&E staining and CD45 (a pan-leukocyte marker for inflammations) IHC staining. The results confirmed that intravaginal topical administration of T512 did not cause nonspecific inflammation in the local cervical tissues and is a safe approach for treating HPV infections and their related diseases.

Discussion

Currently, there is no effective treatment for HPV persistency (26). Prevention of HPV-related cervical cancer relies on costly HPV vaccines and repeated cervical screenings. Although vaccines have shown promising results in recent years, they are all prophylactic, with no therapeutic effects on the existing infections (27). For HPV-infected patients who could not be vaccinated and are still at risk for cervical cancer, repeated screenings and colposcopy-directed biopsies are taken. As a consequence, these interventions give rise to potential overtreatment, additional costs, patient anxiety, and adverse effects (i.e., vaginal bleeding and impaired sexual function) (28). Here, we report that TALEN-mediated genome editing of HPV oncogenes E6/E7 successfully triggered specific apoptosis and growth inhibition and reduced tumorigenicity of HPV-infected cells both in vitro and in vivo. One mechanism of TALEN's therapeutic effects is that TALENs specifically recognize and cleave HPV DNA sequence in host cells, generating DSBs that directly induce apoptosis and suppress proliferation (29). The higher HPV DNA copy number in host cells, the more prominent the genotoxicity of DSBs will become and the more likely the host cells will be selectively killed by the artificially engineered nuclease. Another mechanism by which TALENs exert their therapeutic effect is that, if host cells survive the genotoxic events, they would react and repair the double-stranded DNA breaks via the nonhomologous end-joining pathway (Figure 1A), leading to mutations of *E6/E7* and restored functions of E6/E7-inhibited tumor suppressor p53/RB1 (Figure 3, G–J). The consequence of the chain reaction is the reversal of the malignant phenotype of HPV-infected cells and the reduction of persistent HPV infections (Figure 3, C–F). Together, our data highlight genome editing of HPV oncogenes *E6/E7* by TALENs as an approach for treatment of HPV persistence and infection-associated cervical carcinoma.

Interestingly, we found that intravaginally topical application of TALENs serves as an attractive approach for genome editing of HPV oncogenes *E6/E7*. By applying HPV16-*E7*–targeted TALENs directly to the cervixes of K14-HPV16 transgenic mice, we observed that TALENs effectively induced mutations in the *E7* oncogene and subsequently caused a reduction in the HPV16

DNA load (Figure 4). Further, disruption of the *E7* gene recovered the expression level of RB1 as well as that of its downstream targets CDK2 and E2F1, thereby reversing the cervical malignancy in vivo (Figure 6). Compared with systemic drug administration or oral drug delivery, intravaginally regional administration of TALENs has several unique advantages: first, it provides high concentrations of TALENs acting locally at the target sites and minimizes the potential of systemic side effects; second, it avoids hepatic first-pass metabolism and enzymatic digestion associated with oral administration or the pain and risk of infection caused by systemic administration (i.e., needle injection); and, third, it offers the ease of self-application and removal, which would make it highly acceptable for both patients and doctors. However, many more experiments need to be performed to optimize the efficacy of TALEN-mediated HPV *E6/E7* editing. For instance, in this study, mice were first anesthetized and kept in the dorsal position for at least 40 minutes under anesthesia to avoid loss of the complexes and to achieve efficient transfection effects (Supplemental Figure 13). When applied to human subjects, the length of time that the complexes need to stay resident in the vagina must be further determined. And to extend such time, polymer-complexed TALEN plasmids could be directly applied to the anogenital tract using devices such as the CerviPrep drug delivery system (30) or they could be formulated into vehicles suitable for anogenital tract retention (e.g., suppository, gel, or cream) (31). In addition, physiological changes of the vagina and cervix with the menstrual cycle, particularly the pH value and the vaginal fluid, should also be taken into consideration when TALENs are delivered intravaginally (32).

The specificities and toxicities of TALEN-based genome editing therapy are always the primary concerns for their application in human subjects. Our in vitro and in vivo data proved that the therapeutic effects of HPV *E6/E7*–targeted TALENs were specific enough not only to differentiate HPV-infected cells from natural uninfected cells but also to distinguish host cells infected with different subtypes of HPVs (Figure 2, A and B). We speculate that the longer DNA-binding sequence of TALENs (approximately 30–40 nucleotides or more) determines their improved specificity over clustered regularly interspaced short palindromic repeat (CRISPR) RNA-guided nuclease (33), ZFN, and siRNAs. For example, the specificity of the newly developed, RNA-guided CRISPR endonuclease is mainly determined by the protospacer adjacent motif (2 nucleotides) and seed sequences (approximately 12 nucleotides) that are located at 3′ end of its recognition sequence GN20GG (34). The relatively short length of the CRISPR recognition sequence (approximately 14 nucleotides) makes the endonuclease more prone to produce undesired, off-target mutations in the human genome, thus limiting its further use in therapeutic applications (35). Nevertheless, the specificity of the CRISPR system was recently improved by the paired RNA guided, double-nicking strategy (approximately 28 nucleotides) (36). Therefore, future studies are warranted to investigate the efficacy and specificity of the double-nicking strategy in our cellular and animal models. Similarly, ZFNs could be engineered to target HPV oncogenes. The lengths of these recognition sequences are determined by the number of zinc fingers that constitute the corresponding nuclease (approximately 18–24 nucleotides for 6 to 8 fingers). Although increasing the number of zinc fingers would improve their specificity comparable to that of the TALENs, extensive experiments would be required to screen the best combinations of ZFN monomers with different zinc finger numbers (18).

Our data suggest that TALEN-based antiviral therapy may play valuable roles in HPV-related cervical carcinogenesis. For precancerous stages, such as persistent HPV infections and their related CINs, if appropriately combined with HPV testing, patients would be able to first undergo HPV testing to determine the HPV subtype(s) and then select corresponding type-specific TALENs to treat the appropriate HPV infection(s). These patients would benefit from this new "screen-and-immediately-treat" strategy, in lieu of undergoing repeated screenings (37). Even with advanced cervical cancer, regionally delivered TALEN antiviral therapy may still offer a complementary therapy that could be combined with standard surgery, radiotherapy, and chemotherapy to further eradicate HPV infections and the residual tumor cells. Inhibition of viral E6 and E7 functions would be similar to androgen deprivation therapy for prostate cancer (38). Experiments are currently being carried out to test these hypotheses in our laboratory.

In summary, our data demonstrate that TALENs can effectively disrupt the viral DNA in the host genome, reduce HPV viral load, and reverse the malignant phenotype of infected cells both in vitro and in vivo. TALEN-based antiviral therapy provides a strategy for the treatment of existing HPV infections and their related cervical malignancy.

Methods

Experimental design. Screening of TALENs with different DNA-binding sites using SSA assays was carried out in a blinded fashion, i.e., the plasmids that were used were unknown to the implementers. All of these experiments were performed in triplicate. For cell apoptosis, Western blotting, and the T7EI assay in cell lines, 2 replicates were performed on separate days.

For the T7EI assays in cell lines and, thereafter, experiments on apoptosis, growth curves, Western blotting, and FISH in cell lines, we calculated the IC_{50} by transfecting a series of concentrations of paired plasmids into cells for 72 hours. We ultimately selected an IC_{50} of 48 hours, because growth inhibition was maximized at approximately 48 hours and continued until 72 hours.

For in vivo studies, the sample sizes were determined with the object of minimizing the number of mice required, while still obtaining a statistically significant result, and animals were selected randomly for each group. Animal studies were not blinded to the person performing treatment administration, but they were blinded to the people performing H&E, IHC, and FISH assays in the K14-HPV16 transgenic mice.

Animals. For the xenograft tumor studies, 6- to 8-week-old female BALB/c-nu mice were purchased from Beijing HFK Bio-technology Co. Ltd and housed at the Experimental Animal Center, Tongji Medical College, HUST. The nude mice were grouped randomly, and 6 mice per group were housed at 3 mice per cage. Cells were trypsinized, counted, and resuspended in 100 μl Dulbecco's PBS and injected subcutaneously.

K14-HPV16 transgenic mice have been described previously (21). Breeding pairs of K14-HPV16 transgenic mice were provided by

the National Cancer Institute (NCI) Mouse Repository (Frederick, Maryland, USA) [strain nomenclature: FVB.Cg-Tg(KRT14-HPV16) wt1Dh] and bred at the Experimental Animal Center, HUST. Breeding and genotyping of the offspring is described elsewhere in detail (39). HPV16-positive female mice (6 to 8 weeks old) were randomly grouped. The DNA of TALEN plasmids was complexed with Turbo-Fect In Vivo Transfection Reagent (R0541, Fermentas, Thermo Scientific) according to the manufacturer's protocol. Mice were anesthetized with 3% pentobarbital sodium (intraperitoneal injection of 50 mg/kg mice body weight), and the polymer-DNA complexes were pipetted into the vagina using 200 μl pipet tips after washing with saline (in a maximum volume of 20 μl) (40). Then, mice were kept in the dorsal position for at least 40 minutes under anesthesia to avoid loss of the complexes (Supplemental Figure 12). The mice were euthanized after pentobarbital anesthetization at the indicated times. The vagina was dissected, fixed in 4% paraformaldehyde, and sectioned for IHC.

Plasmids and TALEN assembly. HPV16 expression plasmid was a gift from Harald zur Hausen (German Cancer Research Center, University of Heidelberg, Heidelberg, Germany). GZF1-RR/GZF3-DD and SSA rep3-1 reporter plasmids were gifts from David J. Segal (Department of Pharmacology and Genome Center, University of California, California, USA). Plasmids CAG-mRFP and the Golden Gate TALEN and TAL Effector Kit 2.0 were purchased from Addgene. Plasmid pEGFP-C1 was purchased from Clontech. The full-length HPV16 and HPV18 E6 and E7 sequences were scanned for potential TALEN-binding sites using the online software tool TAL Effector-Nucleotide Targeter (TALE-NT, http://boglabx.plp.iastate.edu/TALENT/). The protocol for the assembly of the TALENs targeting HPV16 and HPV18 E7 was described previously (13). The module and array plasmids of each TALEN were ultimately constructed into pcDNA3.1(+) backbone plasmid (V790-20, Invitrogen), and the sequences of each TALEN are provided in Supplemental Table 1. The amino acid sequences of the *Fok*I variants are listed in Supplemental Note 1.

Cell culture and transfection. The HEK293 and the human cervical cancer cell lines HeLa, SiHa, and C33A were purchased from the ATCC and authenticated at Shanghai Paternity Genetic Testing Center in June 2012 using short tandem repeat DNA profiling (ABI 3130xl Genetic Analyzer, Life Technologies). All cells were maintained in DMEM (Invitrogen) supplemented with 10% FBS (Gibco) and 100 U/ml penicillin and streptomycin (Invitrogen) at 37°C in a humidified incubator with 5% CO_2. The immortalized human cervical keratinocyte cell line S12 was a gift from Kenneth Raj (Centre for Radiation, Chemical and Environmental Hazards, Health Protection Agency, Chilton, Didcot, United Kingdom), and acquisition of the cell line was permitted by the original owner, Margaret Stanley (Department of Pathology, University of Cambridge, Cambridge, United Kingdom) (41). S12 cells were cultured in a 1:3 mixture of DMEM and Ham F-12 medium supplemented with 5% FBS (Gibco), 5 μg/ml insulin (Sigma-Aldrich), 8.4 ng/ml cholera toxin (Sigma-Aldrich), 24.3 μg/ml adenine (Sigma-Aldrich), 0.5 μg/ml hydrocortisone (Sigma-Aldrich), and 10 ng/ml epidermal growth factor (Peprotech). All cells were transfected using the X-tremeGENE HP DNA Transfection Reagent (Roche) according to the manufacturer's instructions. The ratio of the reagent to DNA for each cell line was optimized in preliminary experiments. The experiments were performed in triplicate and repeated twice.

Reporter system assay. HEK293 cells were seeded in a 24-well plate that was incubated overnight at 37°C and then transfected using the X-tremeGENE HP DNA Transfection Reagent (Roche) according to the manufacturer's instructions. For the SSA reporter system, the transfection cocktails included 100 ng of reporter plasmid or pGL3-Ctrl positive control plasmid, 400 ng of each TALEN plasmid, and 25 ng of pRL *Renilla* Luciferase Reporter Vector (Promega), which encoded *Renilla* luciferase. The cells were lysed 48 hours later after transfection in 1′ Passive Lysis Buffer (Promega), and the *firefly* and *Renilla* luciferase activities were measured using a luminometer (BioTek) and the Dual-Luciferase Reporter Assay System (Promega) according to the manufacturer's instructions. The experiments were performed in quadruplet and repeated twice.

The surrogate reporter system has been reported previously (17). Oligonucleotides that contained the target sites were synthesized (GENewIZ) and connected to a constitutively expressed mRFP and an out-of-frame, functional EGFP. The transfection cocktails included 200 ng of reporter plasmid and 400 ng of each TALEN plasmid, and 200 ng of the pEGFP-C1 or CAG-mRFP plasmids were used as negative controls. The fluorescence intensity was detected using a FACSCalibur flow cytometer (BD) and analyzed using the CellQuest Pro software (BD).

T7EI assay. The T7EI assay was performed as previously described (42). Briefly, genomic DNA was extracted from cells using the DNeasy Blood & Tissue Kit (QIAGEN) according to the manufacturer's handbook. The fragments (approximately 500 bp) of genomic regions that encompassed the TALEN target sites were amplified, purified, melted, and annealed. Then, the heteroduplex DNA (200 ng) was treated with T7EI (10 units, M0302S, New England BioLabs) for 15 minutes at 37°C and then analyzed on a 10% TBE polyacrylamide gel. The amplified primers are provided in Supplemental Table 3.

Western blotting and antibodies. Cells were lysed in a buffer containing 50 mM Tris (pH 7.4), 150 mM NaCl, 1% Triton X-100, 1% sodium deoxycholate, 0.1% SDS, and protease inhibitor cocktail (Beyotime). The primary antibodies used for Western-blotting analysis included rabbit anti–HPV16-E6 (1:200, orb10837, Biorbyt), rabbit anti–HPV16-E7 (1:200, orb10573, Biorbyt), mouse anti–HPV18-E6 (1:100, sc-460, Santa Cruz), mouse anti–HPV18-E7 (1:100, sc-51952, Santa Cruz), rabbit anti-RB1 (1:1,000, 10048-2-Ig, ProteinTech), rabbit anti-p53 (1:1,000, 10442-1-Ap, ProteinTech), rabbit anti-CDK2 (1:300, 10122-1-Ap, ProteinTech), and mouse anti-GAPDH (1:1,000, AM1020a, Abgent).

IHC staining. Mice uteruses and cervixes were isolated after the mice were euthanized at the programmed times. Fixed (4% paraformaldehyde) and paraffin-embedded sections (5 μm) were subjected to IHC staining according to the Proteintech protocol (http://www.ptglab.com/Support/index.aspx). The slides were incubated overnight at 4°C with the primary antibody rabbit anti–HPV16-E7 (1:100, orb10573, Biorbyt), rabbit anti-RB1 (1:100, 10048-2-Ig, ProteinTech), rabbit anti-CDK2 (1:200, ab6538, Abcam), rabbit anti-Ki67 (1:100, ab16667, Abcam), rabbit anti-E2F1 (1:100, 12171-1-Ap, ProteinTech), or anti-CD45 (1:100, 103101, Biolegend). Antibody detection was performed using DAB. The typical images were photographed using cellSens Dimension (version 1.8.1, Olympus), and the staining intensity was measured using ImagePro Plus (version 6.0, Media Cybernetics).

FISH. For FISH in cell lines, the sample preparation and hybridization protocol followed that of Garimberti et al. (43). For FISH in paraffin-embedded slides, the hybridization protocol followed that of Summersgill et al. (44). The paraffin-embedded slides were dewaxed, pretreated with NaSCN, digested with pepsin, and hybridized with the HPV16 probe. The HPV16 probe was constructed by nick translation of the HPV16 plasmid with digoxigenin and detected

using peroxidase-conjugated sheep anti-digoxigenin Fab fragments (1:200, 11207733910, Roche) and FITC-labeled tyramide (1:50, NEL701A001KT, Perkin Elmer). Digital images were obtained using an Olympus BX53 fluorescence microscope that was equipped with FITC and DAPI filters.

Statistics. Analysis was performed using SPSS 12.0. Data were presented as mean ± SD. A 2-tailed Student's *t* test was used to determine significance between the treated and control groups. A *P* value of less than 0.05 indicated a significant difference between 2 groups.

Study approval. All experimental protocols were approved by the IACUC of HUST, and the study was carried out in strict accordance with the Animal Research: Reporting In Vivo Experiments (ARRIVE) guidelines (45).

Acknowledgments

We thank H. zur Hausen for providing the HPV16 plasmid; K. Raj and M. Stanley for providing the S12 cell line; D.J. Segal for providing the GZF1-RR/GZF3-DD and SSA rep3-1 plasmids; J.M. Arbert, D. Hanahan, and the NCI Mouse Repository for providing FVB.Cg-Tg(KRT14-HPV16)wt1Dh mice; and Shunchang Zhou for technical support regarding mice reproduction and breeding. This work was supported by funds from the National Development Program (973 Program) For the Key Basic Research of China (2015CB553903, 2013CB911304, and 2009CB521806) and the National Natural Science Funding of China (81372805, 81090414, 81301126, 81402158, 81471508, 81101971, 81402159, 81272859, 81372801, 81302266, 81372806, 81370469, 81403166, 81172466, 81101964, 81172468, 81230052, and 81230038).

Address correspondence to: Ding Ma or Hui Wang, Cancer Biology Research Center, Tongji Hospital, Tongji Medical College, Huazhong University of Science and Technology, 1095 Jiefang Road, Wuhan 430030, Hubei, China. Phone: 86.27.83662681; E-mail: dma@tjh.tjmu.edu.cn (D. Ma), huit71@sohu.com (H. Wang).

1. Jemal A, Bray F, Center MM, Ferlay J, Ward E, Forman D. Global cancer statistics. *CA Cancer J Clin*. 2011;61(2):69–90.
2. Crosbie EJ, Einstein MH, Franceschi S, Kitchener HC. Human papillomavirus and cervical cancer. *Lancet*. 2013;382(9895):889–899.
3. Werness BA, Levine AJ, Howley PM. Association of human papillomavirus types 16 and 18 E6 proteins with p53. *Science*. 1990;248(4951):76–79.
4. zur Hausen H. Papillomaviruses and cancer: from basic studies to clinical application. *Nat Rev Cancer*. 2002;2(5):342–350.
5. Narisawa-Saito M, Kiyono T. Basic mechanisms of high-risk human papillomavirus-induced carcinogenesis: roles of E6 and E7 proteins. *Cancer Sci*. 2007;98(10):1505–1511.
6. Spangle JM, Munger K. The HPV16 E6 oncoprotein causes prolonged receptor protein tyrosine kinase signaling and enhances internalization of phosphorylated receptor species. *PLoS Pathog*. 2013;9(3):e1003237.
7. Arroyo M, Bagchi S, Raychaudhuri P. Association of the human papillomavirus type 16 E7 protein with the S-phase-specific E2F-cyclin A complex. *Mol Cell Biol*. 1993;13(10):6537–6546.
8. McIntyre MC, Ruesch MN, Laimins LA. Human papillomavirus E7 oncoproteins bind a single form of cyclin E in a complex with cdk2 and p107. *Virology*. 1996;215(1):73–82.
9. Dyson N, Howley PM, Munger K, Harlow E. The human papilloma virus-16 E7 oncoprotein is able to bind to the retinoblastoma gene product. *Science*. 1989;243(4893):934–937.
10. Sima N, et al. RNA interference against HPV16 E7 oncogene leads to viral E6 and E7 suppression in cervical cancer cells and apoptosis via upregulation of Rb and p53. *Apoptosis*. 2008;13(2):273–281.
11. Wang W, et al. Selective targeting of HPV-16 E6/E7 in cervical cancer cells with a potent oncolytic adenovirus and its enhanced effect with radiotherapy in vitro and vivo. *Cancer Lett*. 2010;291(1):67–75.
12. Szczepek M, Brondani V, Buchel J, Serrano L, Segal DJ, Cathomen T. Structure-based redesign of the dimerization interface reduces the toxicity of zinc-finger nucleases. *Nat Biotechnol*. 2007;25(7):786–793.
13. Cermak T, et al. Efficient design and assembly of custom TALEN and other TAL effector-based constructs for DNA targeting. *Nucleic Acids Res*. 2011;39(12):e82.
14. Miller JC, et al. A TALE nuclease architecture for efficient genome editing. *Nat Biotechnol*. 2011;29(2):143–148.
15. Doyon Y, et al. Enhancing zinc-finger-nuclease activity with improved obligate heterodimeric architectures. *Nat Methods*. 2011;8(1):74–79.
16. Guo J, Gaj T, Barbas CF 3rd. Directed evolution of an enhanced and highly efficient FokI cleavage domain for zinc finger nucleases. *J Mol Biol*. 2010;400(1):96–107.
17. Kim H, Um E, Cho SR, Jung C, Kim H, Kim JS. Surrogate reporters for enrichment of cells with nuclease-induced mutations. *Nat Methods*. 2011;8(11):941–943.
18. Perez-Pinera P, Ousterout DG, Brown MT, Gersbach CA. Gene targeting to the ROSA26 locus directed by engineered zinc finger nucleases. *Nucleic Acids Res*. 2012;40(8):3741–3752.
19. Kim S, Kim D, Cho SW, Kim J, Kim JS. Highly efficient RNA-guided genome editing in human cells via delivery of purified Cas9 ribonucleoproteins. *Genome Res*. 2014;24(6):1012–1019.
20. Kim JM, Kim D, Kim S, Kim JS. Genotyping with CRISPR-Cas-derived RNA-guided endonucleases. *Nat Commun*. 2014;5:3157.
21. Arbeit JM, Munger K, Howley PM, Hanahan D. Progressive squamous epithelial neoplasia in K14-human papillomavirus type 16 transgenic mice. *J Virol*. 1994;68(7):4358–4368.
22. Grau J, Boch J, Posch S. TALENoffer: genome-wide TALEN off-target prediction. *Bioinformatics*. 2013;29(22):2931–2932.
23. Moody CA, Laimins LA. Human papillomavirus oncoproteins: pathways to transformation. *Nat Rev Cancer*. 2010;10(8):550–560.
24. Moscou MJ, Bogdanove AJ. A simple cipher governs DNA recognition by TAL effectors. *Science*. 2009;326(5959):1501.
25. Boch J, et al. Breaking the code of DNA binding specificity of TAL-type III effectors. *Science*. 2009;326(5959):1509–1512.
26. Sudenga SL, Shrestha S. Key considerations and current perspectives of epidemiological studies on human papillomavirus persistence, the intermediate phenotype to cervical cancer. *Int J Infect Dis*. 2013;17(4):e216–e220.
27. Kahn JA. HPV vaccination for the prevention of cervical intraepithelial neoplasia. *N Engl J Med*. 2009;361(3):271–278.
28. Flanagan SM, Wilson S, Luesley D, Damery SL, Greenfield SM. Adverse outcomes after colposcopy. *BMC Womens Health*. 2011;11:2.
29. Kaina B. DNA damage-triggered apoptosis: critical role of DNA repair, double-strand breaks, cell proliferation and signaling. *Biochem Pharmacol*. 2003;66(8):1547–1554.
30. Hodge LS, et al. Localized delivery of chemotherapy to the cervix for radiosensitization. *Gynecol Oncol*. 2012;127(1):121–125.
31. Gupta S, Gabrani R, Ali J, Dang S. Exploring novel approaches to vaginal drug delivery. *Recent Pat Drug Deliv Formul*. 2011;5(2):82–94.
32. Srikrishna S, Cardozo L. The vagina as a route for drug delivery: a review. *Int Urogynecol J*. 2013;24(4):537–543.
33. Cong L, et al. Multiplex genome engineering using CRISPR/Cas systems. *Science*. 2013;339(6121):819–823.
34. Mali P, et al. RNA-guided human genome engineering via Cas9. *Science*. 2013;339(6121):823–826.
35. Fu Y, et al. High-frequency off-target mutagenesis induced by CRISPR-Cas nucleases in human cells. *Nat Biotechnol*. 2013;31(9):822–826.
36. Ran FA, et al. Double nicking by RNA-guided CRISPR Cas9 for enhanced genome editing specificity. *Cell*. 2013;154(6):1380–1389.
37. Denny L, et al. Screen-and-treat approaches for cervical cancer prevention in low-resource settings: a randomized controlled trial. *JAMA*. 2005;294(17):2173–2181.
38. Perlmutter MA, Lepor H. Androgen deprivation therapy in the treatment of advanced prostate cancer. *Rev Urol*. 2007;9(suppl 1):S3–S8.
39. Sepkovic DW, Stein J, Carlisle AD, Ksieski HB, Auborn K, Bradlow HL. Diindolylmethane inhibits cervical dysplasia, alters estrogen metabolism, and enhances immune response in the K14-

HPV16 transgenic mouse model. *Cancer Epidemiol Biomarkers Prev*. 2009;18(11):2957–2964.
40. Palliser D, et al. An siRNA-based microbicide protects mice from lethal herpes simplex virus 2 infection. *Nature*. 2006;439(7072):89–94.
41. Stanley MA, Browne HM, Appleby M, Minson AC. Properties of a non-tumorigenic human cervical keratinocyte cell line. *Int J Cancer*. 1989;43(4):672–676.
42. Reyon D, Tsai SQ, Khayter C, Foden JA, Sander JD, Joung JK. FLASH assembly of TALENs for high-throughput genome editing. *Nat Biotechnol*. 2012;30(5):460–465.
43. Garimberti E, Tosi S. Fluorescence in situ hybridization (FISH), basic principles and methodology. *Methods Mol Biol*. 2010;659:3–20.
44. Summersgill BM, Shipley JM. Fluorescence in situ hybridization analysis of formalin fixed paraffin embedded tissues, including tissue microarrays. *Methods Mol Biol*. 2010;659:51–70.
45. Kilkenny C, Browne WJ, Cuthill IC, Emerson M, Altman DG. Improving bioscience research reporting: the ARRIVE guidelines for reporting animal research. *PLoS Biol*. 2010;8(6):e1000412.